**A Thesis**

**On**

# Synthesis & characterization of Non-Lead based multiferroic composites

***Submitted in partial fulfillment of the requirement for***

***The award of degree of***

**Master of Science (Physics)**

**Submitted by**

**Amritpal**

**Roll No. 301304001**

**Supervisor**

**Dr. Puneet Sharma**

**Associate Professor**

**Under**

**School of Physics and Materials Sciences**

**Thapar University**

**Patiala-147004**

**July 2015**

*I dedicate my thesis to my loving family, friends and my brother*

*Harpreet Singh who have always been supportive toward me.*

# *Certificate*

This is to certify that the report entitled "The synthesis and characteristics of Non-Lead based multiferroic composites" submitted by **Amritpal, Roll No. 301304001**, student of (M.Sc.) in Physics, School of Physics & Materials Science, Thapar University, Patiala, was carried out by her under my supervision. She has not submitted this material towards any degree at Thapar University, Patiala or any other university.

**(Dr. Puneet Sharma)**

**Supervisor**

**Associate Professor**

**School of Physics & Material Science**

**Thapar University, Patiala - 147 004**

**Countersigned by:**

**( Dr. Manoj K. Sharma)**

**Head &Associate Professor**

**School of Physics & Material Sciene**

**Thapar University, Patiala - 147 004**

**( Dr. S.S Bhatia)**

**Dean, Academic Affairs,**

**Thapar University,**

**Patiala - 147 004**

# *Acknowledgement*

I express my deep sense of gratitude and respect to **Dr. Puneet Sharma, Associate Professor, School of Physics and Material Science, Thapar University, Patiala** my guide for his keen interest and valuable guidance, strong motivation and constant encouragement during the course of the work. I thank him for his great patience, constructive criticism and many useful suggestions apart from invaluable guidance to me. I am sure that the knowledge gained through my association with my supervisor will help me in future.

I am thankful to **Mr. Mintu Tyagi** for their kind help and suggestions at every stage of my project report work.

I am also thankful to **Mrs. Samiksha Verma, Mrs. Shivani Sharma, Mr. Anoop Pratap Singh and Ms. Chhavi Pahwa** and **my friends** for their help and support at every stage during the project report work.

I would also like to thank **Mr. Angrej Gill** for supporting and encouraging me with his best wishes.

Finally, I would like to express my deepest gratitude to **my parents**, without whom I am nothing, to provide me great opportunities, everlasting support big encouragement and lots of love.

Amritpal

**Amritpal**

# *Abstract*

Multiferroic materials are of particular interest due to their long range of applications in sensors, phase shifters, transducers, and memory devices. Non-Lead based *ME* composites have recently drawn increasing interest because they are non-toxic in nature and environmental friendly.

Pure BNT-BKT-BMgT and CZFMO and composite BNT-BKT-BMgT-CZFMO have been prepared by using sol-gel technique. The structural, magnetic, ferroelectric and morphological properties have been investigated and discussed.

The study of ferroelectric behavior of pure BNT-BKT-BMgT and composites show the decrease value of saturation polarization for composite are observed due to low resistivity of ferrite phase.

The magnetic study of pure CZFMO and composites 72.5BNT-22.5BKT-5BMgT show the well saturated *M-H* loop indicates the ferromagnetic nature of samples. The corecivity of the sample increased from ~ 260 Oe for pure CZFMO to ~ 48 Oe for composite (x=0.2). The corecivity of the samples confirmed the soft magnetic nature of the sample.

**List of Figures** **Page No.**

# CONTENTS

## CHAPTER 1

## INRODUCTION

### 1.1 Multiferroic materials

The materials which exhibit simultaneously two or more ferroic order parameters are called multiferroics [1-5]. In 1994, **Schmidt** first discovered the term multiferroics [6]. In multiferroics materials, the different order parameters coupled together to produce the new effect known as the Magneto-electric effect [7, 8]. The magneto electric coupling is the induction of electric polarization by magnetic field or the induction of the magnetization by electric field. When the electric polarization P appears by applying a magnetic field H, this is known as the direct *ME* effect is given by the relation

$$\Delta P = \alpha_E \Delta H$$

Where E denotes the electric field and $\alpha_E$ is the *ME* coefficient. In contrast Magnetization M appears by applying an electric field E, this is known as the converse *ME* effect given by the relation:

$$\Delta M = \alpha_E \Delta E$$

Recently, magneto electric multiferroic materials are particularly interest due to their wide range of applications in phase shifters, sensors and transducers. The relationship between the multiferroics and magnetoelectric pictorially depicted by several authors using the schematic diagram as shown in fig. 1.1

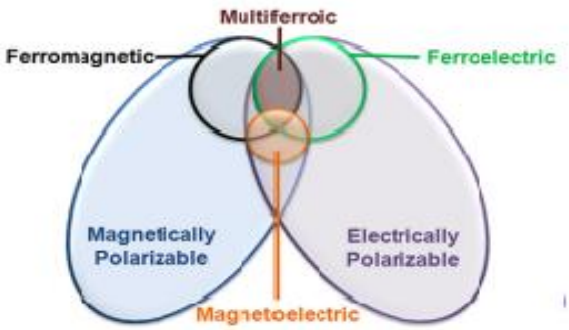


**Fig: 1.1** The relationship between multiferroics and magnetoelectric materials [9].

The multiferroic *ME* materials can be divided into two types

### 1.2 Single phase multiferroics

Single phase multiferroics are materials which possesses two or more of the ferroic properties. Naturally occurring multiferroic single phase compounds are very scarce. The low temperature intrinsic *ME* effect exist in the single-phase materials hinder their practical applications in memory devices. $BiFeO_3$ and rare earth manganates are the examples of single phase multiferroic materials [10-17]. Single phase multiferroics are further divided into two groups.

#### 1.2.1 Type-I single phase multiferroics

Type-I single phase multiferroic materials are basically the perovskite compound in which origin of the ferroelectricity and magnetism are independent. The large value of polarization of the order (10-100 $\mu C/cm^2$) appears at room temperature make them useful for practical applications. Examples of type-I single - phase multiferroic materials are $BiMnO_3$, $BiFeO_3$, $YMnO_3$ etc [18-24]. There are many sources of ferroelectricity in such materials.

**Ferroelectricity due to lone pair**

$Bi^{3+}$and $Pb^{2+}$ in $BiMnO_3$ and $PbVO_3$plays a very important role in the production of ferroelectricity. There are two electrons in s orbital of one of the cation which are far from the core and they do not participate in the chemical bonds. They are called the lone pairs or the dangling bonds. The origin of ferroelectricity in these compounds can be explained by ordering of these lone pairs in one direction.

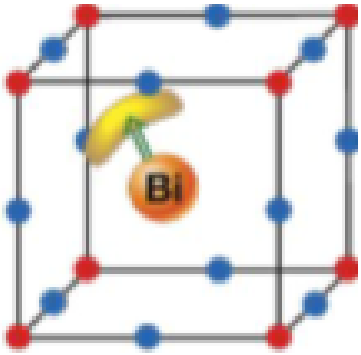


**Fig: 1.2.** Lone pair of $Bi^{3+}$ [25]

**Ferroelectricity due to charge ordering**

Charge ordering can occur in transition metal compounds which have the similar cations at same structural sites but with different valence. Ferroelectricity can be induced by charge ordering when inequivalent bonds are created between sites having different charges. The inequivalent sites lead to ferroelectricity [26]. Example of charge ordered multiferroics are $TbMn_2O_5$, $LuFe_2O_5$.

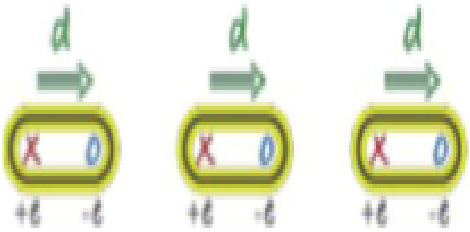


**Fig: 1.3.** Inequivalent sites lead to ferroelectricity [25]

**Geometric ferroelectricity**

At higher temperature, the structural phase transition causes the geometrical ferroelectricity. The compounds belong to this class are hexagonal magnetises such as $RMnO_3$. Ferroelectricity in $YMnO_3$ has nothing to do with magnetic $Mn^{3+}$ but it occurs due to the tilting of $MnO_5$ polyhedrons which gives a closed packing, as a result oxygen ions moves closer to rather small Y ions [27].

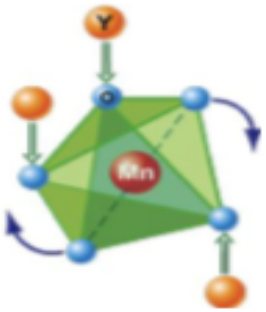


**Fig: 1.4.** Tilting of $MnO_5$ with magnetic Mn [25]

### 1.2.2 Type – II single phase multiferroics

The second type of single phase multiferroics is classified as Type-II single phase multiferroics. Materials of this group show the smaller polarization values ~ $10^{-2}$ μC/cm$^2$. In $TbMnO_3$, magnetic ordering appears at $T_{N1}$ = 41K and the second magnetic transition at $T_{N2}$ = 28K, magnetic structure changes. Type –II multiferroics can be divided into further two groups, one is the multiferroics in which ferroelectricity caused by particular type of spiral magnetic structure. Examples include $TbMnO_3$ and $MnWO_4$.Other is that in which ferroelectricity is caused by collinear type structure. Example: $Ca_3CoMnO_6$.

## 1.3 Composite multiferroics

Small magnetoelectric coupling in single - phase composites interrupt initial developments in this field and limit their practical applications. So, alternative approaches have been developed to form composites structures with enhanced coupling between the electric and magnetic properties. Magnetoelectric multiferroic composites consist ferroelectric phase and ferromagnetic phase and an artificial coupling is engineered between them through stress mediation at room temperature. In 1972, **Van Suchtelen** firstly proposed the concept of *ME* effect in composites. So, the *ME* effect in composites is resulting from the product of magnetostrictive effect in the magnetic phase and piezoelectric effect in ferroelectric could be written as:

$$\mathrm{ME_H\ effect} = \frac{\text{magnetic}}{\text{mechanical}} \times \frac{\text{mechanical}}{\text{electric}}$$

$$\mathrm{ME_E\ effect} = \frac{\text{electric}}{\text{mechanical}} \times \frac{\text{mechanical}}{\text{magnetic}}$$

Neither of the piezoelectric phase nor magnetostrictive phase has any *ME* effect but when these two component phases are combined in composite structure, the composite exhibits a remarkable *ME* effect. Thus, *ME* effect in composites is extrinsic effect that would depend on the various factors such as composite microstructure and coupling interaction between the two component phases. The higher value of piezoelectric and piezomagnetic coefficients give raise to large *ME* effect in composite system. Various multiferroic composites studied in literature are BT-CFO, BT-NFO, BFO-CFO and BFO-NFO, PZT-NFO, PZT-CFO etc.

On the basis of materials constituents composites are classified as Lead based and Non Lead based multiferroic ME composites as

### 1.3.1 Lead based multiferroic *ME* composites

Pb based piezoelectric ceramics having excellent dielectric and piezoelectric properties are particularly dominant material used as piezoelectric component for preparation of lead based Multiferroic *ME* composites [28-30]. PZT is a lead based extensively studied piezoelectric in literature. However, due to toxic nature of Pb based multiferroic composites presents environmental problem.

### 1.3.2 Non-Lead based multiferroic *ME* composites

To overcome the problem of Pb base materials the focus of researchers has been shifted toward the non lead based materials. Recently, several piezoelectric materials are studied includes BNT, BT, BFO etc. Among them BNT based ferroelectric/piezoelectric materials are particularly interested and have been focused on finding an alternate of lead based piezoelectric materials for preparation of multiferroic *ME* composites. However, high piezoelectric coefficient ($d_{33}$~600pm/V) and high electromechanical coupling coefficient ($k_p$~0.7) of PZT is difficult to match with other non lead based piezoelectric materials [31]

In addition to choices of ferroelectric/piezoelectric component, the selection of magnetic component based on the magnetostriction, resistivity, permeability and chemical stability also important for better performance of *ME* composites. Thus the choice for magnetostrictive materials narrows down toward the spinel ferrites (NFO, CFO) having high values of magnetostriction coefficient and good chemical stability [32-35]**.** In addition to good piezoelectric response as well as magnetostriction coefficient, there are some technical issues suggested by Boomgard *et al.* which can improve the strength of *ME* coupling coefficient in particulate composites addressed like:(1) Adequate interface contact between magnetic and electric order parameter to ensure better mechanical coupling so that the strain expected to be high transferred by magnetic to piezoelectric part.

(2) Reduce chemical reactions at the interface between piezoelectric and piezomagnetic phases during sintering as they are prone to deteriorate *ME* response of composites. Also, in comparison to conventional solid state method the sol-gel derived powders are comparatively fine and provide extra degree of freedom, such as higher density, better interface contact and lattice strain which plays an important role to improved the *ME* coefficient. Particulate composites are easily prepared using the conventional solid state method as well as sol-gel method.

Various recent *ME* composites investigated in recent years, can be divided in groups such as

**1.4 Bulk ceramic composites**

In past decades, bulk ceramic composites were prepared using piezoelectric phase such as $BaTiO_3$, PZT, $PbTiO_3$ and ferrites ($CoFe_2O_4$, $NiFe_2O_4$). The *ME* composites can be prepared by various connectivity schemes such as (0-3), (2-2), (1-3). The (0-3) type particulate composites consist of piezoelectric and magnetic oxide grains, (2-2) type bulk ceramic laminated composites consists of the oxide layers of piezoelectric and magnetic phases. (1-3) type composites consist of the fibres of one phase embedded in the matrix of another phase.

The maximum *ME* coefficient observed in the (2-2) type laminate ceramics is several composites. The research for these materials found that the effective *ME* coefficient for these composites depend upon the composite microstructure, grain shape, volume fraction of two phases, phase connectivity etc.

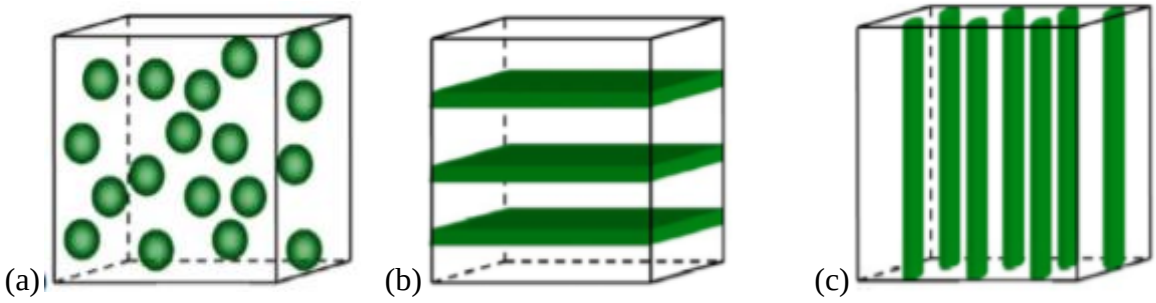


**Fig: 1.5.** Schematic illustration of three bulk composites with three common connectivity schemes: (a) 0-3 particulate composite, (b) 2-2 laminate composite, (c) 1-3 fiber/rod [1]

### 1.5 Nanostructured thin film composites

So far, a number of multiferroics *ME* films of ferroelectric e.g. BTO, $PbTiO_3$ (PTO), PZT and BFO and magnetic e.g. CFO, NFO, LCMO are prepared via physical deposition techniques with different nanostructures such as 0-3 type particulate films, 2-2 type layered heterostructures and 1-3 type vertical heterostructures.

In comparison to bulk *ME* composites, nanostructured thin films have unique properties. Thin film provides more degree of freedom such as lattice strain, which modify the *ME* behaviour. It also provides a way to investigate the physical mechanism of *ME* effect in nanoscale.

### 1.6 Features of Multiferroic *ME* composite

#### 1.6.1 Ferroelectricity

Ferroelectricity is the phenomenon in which spontaneous electric polarization can be switched by applying the external electric field. On applying the electric field, the domains

consisting by the various regions get oriented in the direction of the applied electric field and also this give rise to large change in the polarization value. As saturation is reached, remnant polarization remains in the absence of external electric field. On the basis of symmetry consideration, a crystal structure can be divided into 32 point groups. Out of 32 point groups, 11 crystals classes are centre of symmetric and remaining 21 are non- centrosymmetric. Further, out of 21 non- centrosymmetric point groups 20 are piezoelectric.

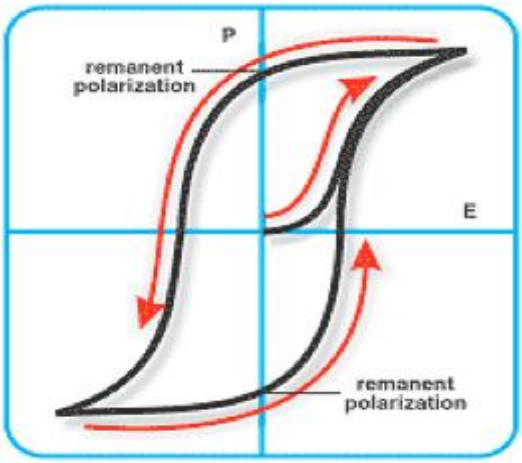


**Fig: 1.6.** Ferroelectric hysteresis loop for a ferroelectric crystal [36]

Among these 20 piezoelectric point groups, 10 groups have a unique polar axis and can be spontaneously polarized, belong to ferroelectric class. The variation in spontaneous polarization with electric field is not linear although it is a closed loop known as the hysteresis loop as shown in fig.1.6. The most widely studied ferroelectric materials are oxides with a perovskite structure of the form $ABO_3$.

### 1.6.2 Piezoelectricity

Piezoelectricity is defined as the applied mechanical stress developed the electric voltage across the material conversely the strain developed across the material if voltage is applied. These effects are known as direct piezoelectric and converse piezoelectric effect respectively. The basic equations representing these two effects can be written as follows

$$\mathbf{D}_i = \mathcal{E}_{ij}^{T} E_i + \mathbf{d}_{ijk} \mathbf{T}_{jk}$$

$$\mathbf{S_{ij} = d_{ijk}E_k + s_{ijkl}\,{}^{E}T_{kl}}$$

Where D is electric displacement vector, E is electric field vector, T is mechanical stress tensor, S is mechanical strain tensor, ‘ε’ is dielectric constant vector,‘d’ is piezoelectric constant tensor and s is mechanical compliance tensor.

### 1.6.3 Ferromagnetism

Ferromagnetism is the phenomenon in which spontaneous magnetization below critical temperature that can be switched and saturated along the direction of applied magnetic field. There is remanent magnetization *($M_r$)* in the absence of applied magnetic field. Pauli Exclusion Principle and electron spin can be used to explain the physical basis of this phenomenon. The spin of electron combines with orbital angular moment to generate the magnetic dipole moment. Presence of the unpaired electrons or partially filled electron shells is a condition for generating spontaneous magnetization in the absence of applied magnetic field. The applications of the ferromagnetism strongly determined by the values of remanent magnetization and corecivity.

## 1.7 Crystal structures

### 1.7.1 Perovskite oxides

The mineral perovskite $CaTiO_3$ was initially found and named after a Russian mineralogist, Count Lev Aleksevich von Perovski. Gustav Rose in 1839 discovered and named it from samples found in the Ural Mountains. Later on, it was used to described a group of oxides having same structures with a general stoichiometry $ABO_3$ where A and B are cations and O is an anion. The A atoms are bigger than B atoms. The cation A is surrounded by 12, O anions and cation B is surrounded by 6 O anions. A is such as $Bi^{3+}$,$Ba^{2+}$ etc. and B is such as $Fe^{3+}$, $Ti^{4+}$ etc. The most symmetric structures observed for $A^{3+}B^{3+}O_3$ perovskite is rhombohedra $R\bar{3}c$ included the rotation of $BO_6$ octahedral with respect to cubic structure.BNT, BFO, PZT are the perovskite materials which are used as a

ferroelectric/piezoelectric components for the preparation of multiferroic *ME* composites in bulk as well as in thin films. The unit cell of such compounds is shown in figure.1.7.

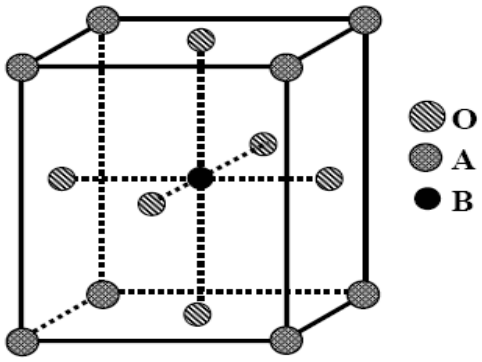


**Fig: 1.7.** Systematic representation of perovskite unit cell [37]

### 1.7.2 Spinel Ferrites

Ferrites are ferrimagnetic metal oxides represented by the general formula $AB_2O_4$, where A is the divalent ion. Ferrites are widely used materials as a piezomagnetic component in *ME* composite preparation for bulk and thin films. Fig. 1.8 shows the crystal structure of spinel ferrite.

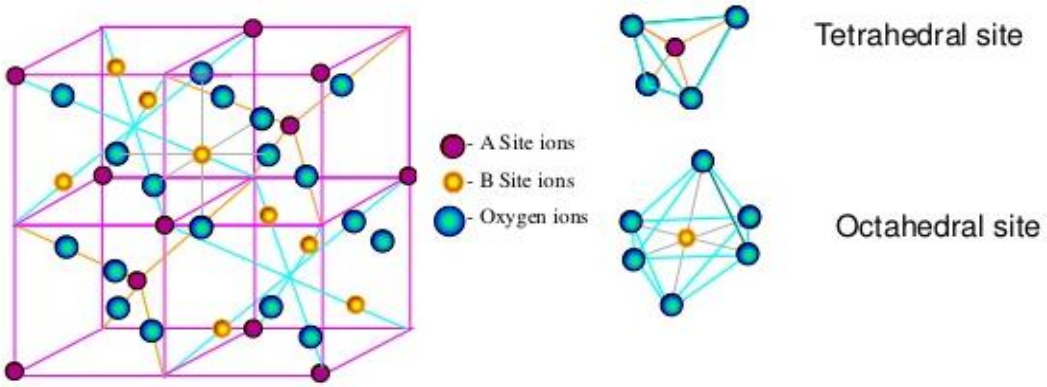


**Fig: 1.8.** Crystal structure of spinel ferrites [38]

### 1.8 Applications of *ME* composites

*ME* composites exhibit large *ME* effect at room temperature that can be successfully utilized for technological applications e.g. magnetic field sensors, phase shifters, transducers etc.

### 1.8.1 *ME* composite as magnetic field sensor

Magnetic field sensing devices can be made by using *ME* composites. On the application of magnetic field, the piezomagnetic components in *ME* composites responds, which in turn, induces a proportional electric charge and makes it better for magnetic field sensor based application.

### 1.8.2 *ME* composite for data storage device

The magneto electric coupling in multiferroic can be used for technological application in electric random access memories (MERAMs). In MERAMs, there is an interfacial exchange coupling between the multiferroic and ferromagnet that can be controlled by electric field which is capable through magnetoelectric coupling. Magnetization of the ferromagnetic layer can be controlled and switched by this coupling. So, finally the magnetization can be controlled by the electric polarization of the multiferroic.

### 1.8.3 *ME* composite for memory device

For memory devices, the *ME* composites can be integrated into semiconductor devices are of particular interest not only in ferroelectric memory devices (FeRAM) but also for ferroelectric field-effect transistors (FeFET-RAM).The *ME* composites based memory devices allow the magnetic data to be written electrically and read magnetically.

## CHAPTER 2

## LITERATURE REVIEW

In 1957, **Landau and Lifshtiz** proposed the existence of *ME* effect in magnetically ordered crystals. In 1959, firstly, the antiferromagnetic materials $Cr_2O_3$ shows the occurrence of *ME* effect which was theoretically predicted by **Dzyaloshinskii** [39]. In1960, **Astrov** also continued the work on *ME* material and confirms the induced magnetization under the influence of electric field in antiferromagnetic $Cr_2O_3$ [40].The magneto-electric multiferroic composites were applicable in transducers, magnetic sensors, actuators etc. In recent years, many efforts has been done in developing of advanced spintronics.

**Y. Lin *et al. 2005*** [41] reported the multiferroic laminated composites of Terfenol-D/polyvinylidene-fluoride (PVDF) and lead-zirconate titanate (PZT) prepared by simple hot – molding technique. The improved magnetoelectric properties were observed for all studied samples. The maximum value of magnetoelectric sensitivity 6V/cm was obtained at 90 kHz for TPT-2 samples.

**Ryu *et al. 2001*** [42] synthesized the magneto electric particulate composites consisting of PZT and Co, Cu, Mn doped Ni-Ferrite ($NiCo_{0.02}Cu_{0.02}Mn_{0.1}Fe_{1.8}O_4$) by conventional ceramic sintering process. Chemical reaction of the PZT with ferrite and connections of ferrite particles make it difficult to get high magnetoelectric effect. The magneto-electric voltage coefficient 115 mV/cm was observed for the composite having 20% ferrite content, which is 44% higher than the other composites prepared in this series.

**J. Zhai *et al. 2004*** [43] fabricated the particulate composites of PZT and $NiFe_2O_4$ by using the conventional ceramic processing. The ME effect of bi-ferroic composites have been studied which is strongly dependent on the volume fraction of NFO . The maximum value of

magnetoelectric coefficient about 80 mV cm$^{-1}$ Oe$^{-1}$ was observed for 0.32 $NiFe_2O_4$/0.68PZT composites. In the low field range, these composites exhibit a very large ME response which varies linearly by varying the both ac and dc magnetic fields.

**Zhai *et al. 2004*** [44] reported the multiferroic laminated composites of $PbZr_{0.53}Ti_{0.47}O_3$ (PZT)/$NiFe_2O_4$ with *ME* sensitivity as high as 0.21 V/A at 11.9 kA/m. Samples have been prepared by a conventional ceramic processing. In low biasing field, these composites exhibit a very large ME sensitivity varying linearly with the magnetic bias which make the composites useful for technological applications of ME device.

**L.Weng *et al. 2007*** [45] prepared the ME composites consisting of $Pb(Zr_{0.48}Ti_{0.52})O_3$ and $COFe_2O_4$ via an ethylenediaminetetraacetic (EDTA)–citrate gel process. Samples were sintered at 1080°C for 1h. In sintered bulk samples, the particles of CFO (1-2μm in size) are embedded in PZT matrix having a grain size of 0.3-0.5μm which leads to a high electrical resistivity (near about $1.8\times10^{11}$ Ω cm). The high electrical resistivity of composites improves the dielectric and ME behaviour of studied sample in present series.

**G. Srinivasan *et al. 2001*** [46] reported on the samples with layer thickness 10-200μm of nickel ferrite and lead zirconate titanate prepared by doctor-blade technique. Stress mediated electromagnetic coupling in bilayers and multilayers of nickel ferrite and lead zirconate titanate gives rise to giant magnetoelectric effect. Value of magneto-electric voltage coefficient was observed in bilayers ranges from 460mV/cmOe to 1500 mV/cm Oe for multilayers.

**Zhou *et al. 2006*** [47] reported $PbZr_{0.52}Ti_{0.48}O_3/CoFe_2O_4/PbZr_{0.52}Ti_{0.48}O_3$ multiferroic laminated composites. The composites were prepared by using conventional ceramic processing. The maximum value of ME voltage coefficient of the composites reaches up to about 27mV/Oe. The dielectric constant of PZT layer is high and CFO layer is low due to

which the relative thickness of the individual phases affect the dielectric behaviour of composites.

**N. Babu *et al. 2011*** [32] synthesized the composites $NiFe_2O_4$ (NFO) and $Na_{0.5}Bi_{0.5}TiO_3$ (NBT) by sol-gel method. XRD pattern confirms the single phase formation of NFO and BNT and two phases in the composites. Dielectric constant and dielectric loss are observed as a function of frequency ranges from 40Hz to 1MHz. The ME response of 0.14% ~ 6kOe at 1 MHz was obtained from the composites 67NFO-33NBT.

**Gupta *et al. 2011*** [34] reported the Mn and Zn simultaneously substituted CFO (CZFMO) posses the highest value of magnetostrictive coefficient. PZT – CZFMO composite samples (diameter ~ 8mm and thickness ~ 1mm) were prepared by using conventional mixed oxide sintering method. The maximum value of magnetoelectric voltage coefficients ~ 122 mV/cm Oe was observed in composite with x = 0.90 at frequency ~ 1 kHz.

**Gupta *et al. 2013*** [35] reported the structural, dielectric, magnetic and magneto electric properties of (1-x) CZFMO - (x) BT of the composites where x = 0.50, 0.60 and 0.70. The highest value of ME voltage coefficient ~ 73 mV/cm Oe was obtained in the sample with x = 0.50. With increasing the content of non-magnetic BT, the value of ME voltage coefficient decrease. Dielectric characteristics of the composite samples show the two anomalies. The low temperature anomaly corresponds to ferroelectric to paraelectric and higher temperature corresponds to magnetic transitions in ferrite.

**S. K. Upadhyay *et al. 2013*** [48] synthesized the ME composites 0.9 $BaTiO_3$ – 0.1 $Ni_xZn_{1-x}Fe_2O_4$ (where x = 0 to 1.0 at an interval of 0.2) by the solid state route. The structural, magnetic and magneto electric measurements were observed. The improvement in magneto-electrical properties is observed via the relative concentration of Ni and Zn in ferrite phase of the composites.

**Srinivas *et al. 2012*** [49] synthesized the ME particulate composite of 65 mol% of $Na_{0.5}Bi_{0.5}TiO_3$ and 35 mol % of $CoFe_2O_4$.Structure, microstructure, ferroelectric, magnetostrictive, magnetic properties of the composites were studied. Variation of magnetization was observed under electrically poled and unpoled conditions. The variation of magnetization under poled condition is -15% at 500 Oe magnetic fields. The value of magnetostriction measurement was obtained as $\lambda_{11} = - 57\times10^{-6}$. The maximum in magneto electric output varied from 1350 mV/cm to 2000 mV/cm with change in electrical poling condition.

**Pradhan *et al. 2013*** [50] studied the magnetic, ferroelectric and dielectric properties of the multiferroic (1-x) $Pb(Fe_{0.5}Nb_{0.5})\ O_3$- (x)$Ni_{0.65}Zn_{0.35}Fe_2O_4$ composites. X-ray and Raman studies confirm the phase formation of the composites. Saturation magnetization, remnant polarization, and coercive field of the composite materials are found to be increase with increasing the value of x but the electrical characterization shows a decrement in remnant polarization and dielectric constant.

**N. Adhlakha *et al. 2012*** [51] synthesized the hybrid composites (1- x)$Ba(Ti_{0.85}Zr_{0.15})O_3$ - (x) $Ni_{0.75}Zn_{0.25}Fe_2O_4$ for x = 0,0.20,0.30 and 0.40 by using the solid state method. The XRD graphs show the formation of spinel- perovskite mixed phase for all prepared compositions. FESEM micrographs determine the dense nature of the samples. The few pores are presented in the homogeneity micrographs. The temperature dependence of the dielectric constant and dielectric loss of the composites measured at three different frequencies 100Hz, 1KHz and 10KHz. The value of dielectric constant is found to be steadily increased with temperature up to transition temperature and then decrease afterwards. The value of remnant polarization for pure BZT is found to be $6.18\mu C\ c\bar{m}^2$. The value of remnant polarization decreases as the content of ferrite phase increased up to 40 mol%. The maximum value of magneto electric effect has been studied using magneto capacitance for 40 mol% addition of ferrite.

**A. D. Sheikh *et al. 2011*** [52] reported the dielectric, multiferroic and magneto electric properties, phase connectivity of (1-x) $Pb(Mg_{1/3}Nb_{2/3})_{0.67}Ti_{0.33}O_3$ and (x) $Ni_{0.8}Co_{0.2}Fe_2O_4$ where x = 0.15, 0.30, 0.45 ME composites prepared by conventional solid-state reaction method. XRD results show the co-existence of NCFO and PMN-PT phases in the composites. The SEM study showed the various types of connectivity schemes such as 3-0, 3-1 and 3-3. The phase transition temperature of PMN-PT is independent of $Ni_{0.8}Co_{0.2}Fe_2O_4$.Ferroelectricity of the ME composites co-related to the different connectivity schemes. Moreover, the 3-3 connectivity obtained with high content of NCFO, forms low-resistivity channels and a large number of dielectric poles remain unaligned. Thus, in the composite NCFO/PMN-PT the good ME response is obtained from the samples consisting PMN-PT while a low ME response from NCFO- rich samples.

**Sreenivasulu *et al. 2009*** [53] reported the (100 – x) $BaTiO_3$ – (x)$NiFe_{1.98}O_4$ (x = 20, 40, 60 and 80 wt%) the nanocomposite exhibit large ME coefficients due to the large piezoelastic strain coefficients and a adequate interface contact between both BT and NF phases. The largest value of $\alpha_E$ = 252 mV $cm^{-1}$ $Oe^{-1}$ was obtained for nanocomposite with x = 40. The effect of size and interface has been studied through microscopy measurements.

**E. Venkata *et al. 2012*** [54] synthesized the CZFMO-NBT-BT composites by the conventional solid state method. X-ray diffraction (XRD), Scanning electron microscope (SEM), Raman spectroscopy, Energy dispersive X-ray spectrometer (EDS), P-E hysteresis loop measurements were used to characterize the samples. Raman spectroscopy shows that the combination of two dissimilar materials could cause a strain in the participating phases of the composites resulting in the shift of Raman modes. The P-E hysteresis loop of NBBT and composites with ratio 85:15 exhibit the saturated loop while the other samples of the series suffers from leakage current. Magnetization measurements on the electrically poled samples showed the strong *ME* coupling due to converse piezoelectric effect.

# CHAPTER 3

# EXPERIMENTAL AND CHARACTERIZATION TECHNIQUES

This chapter give details the processing methods employed for synthesizing the samples of different compositions. A brief detail of various characterization techniques used to study structural, microstructural, and ferroelectric properties are provided. In this work the sol-gel method is adopted to synthesis of sample

The sol-gel method is very simple, cost effective and conventional for synthesis for composites. The processing parameters and the composition required for preparation of samples can be controlled easily using sol-gel method.

## 3.1 Sample preparation

Bismuth nitrate penthydrate [$Bi(NO_3)_3.5H_2O$], Sodium nitrate $Na_2Co_3$, Potassium nitrate $KNO_3$, Magnesium nitrate $Mg(NO_3)_2.6H_2O$, Titanium isoperoxide $TiC_{12}H_{28}O_4$ were used to prepare BNT-BKT-BMgT via sol-gel method. In first step, all the precursors were dissolved in 2-methoxyethanol and citric acid to obtain the solution of BNT-BKT-BMgT. This solution is further stirred and heated at 50°C until the powder formed. Then powder is calcined at 700°C.

In second step, Cobalt nitrate hexahydrate [$Co(NO_3)_2.6H_2O$], Zinc nitrate hexahydrate [$Zn(NO_3)_2.6H_2O$], Iron nitrate nonahydrate [$Fe(NO_3)_2.9H_2O$], Magnesium nitrate hexahydrate [$Mn(NO_3)_2.6H_2O$]were used to prepare CZFMO powder. The prepared powder is calcined at 700°C. In the next step, (1-x) BNT-BKT-BMgT – x CZFMO *ME* composites were prepared by mixing and grinding the BNT-BKT-BMgT and CZFMO powders in desired weight ratio. Mixture of both powders is pressed into cylindrical pallets of diameter 10mm at a pressure of

12.5 MPa. The pallets were sintered at 900°C and used for further measurements such as X-ray diffraction, SEM etc.

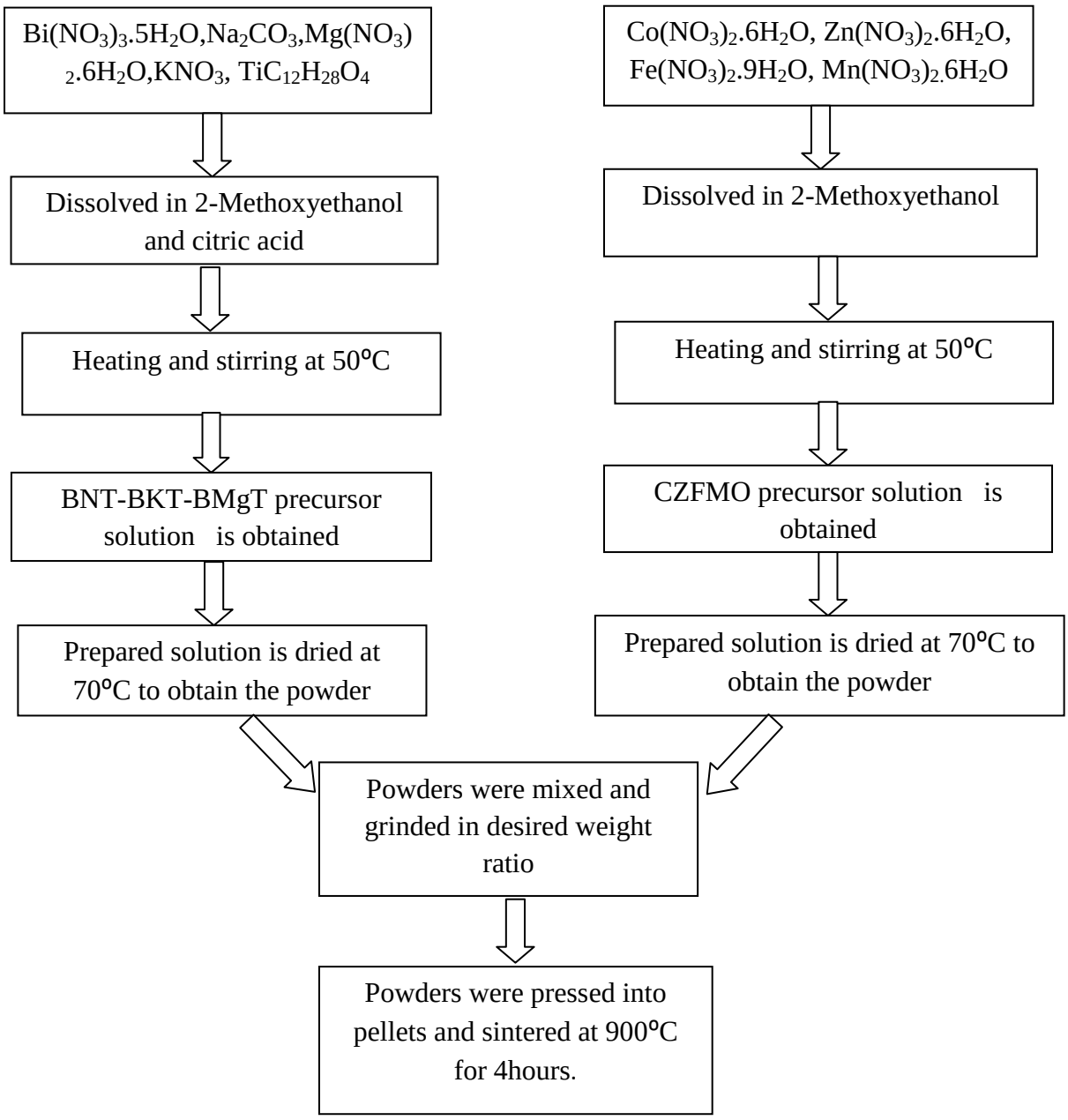


**Fig: 3.1** Flow chart of synthesis of multiferroic composites

### 3.2 Characterization techniques:

The characterization of the materials for the determination of structural analysis, morphological analysis, and magnetic analysis, plays an important role for the quality control and development of advanced materials for device applications. The structural,

compositional, morphological, magnetic and dielectric properties of materials can be characterized by using the techniques such as X-ray diffraction (XRD), Scanning Electron Microscopy (SEM), Vibrational Sample Magnetometer (VSM), Energy dispersive X-ray spectroscopy (EDS).

### 3.2.1 X-Ray diffraction:

X-ray diffraction (XRD) is a fast non-destructive analytical technique that reveals the detailed of information about the chemical composition and crystallographic structure of synthesized materials. The phenomenon of diffraction of X-rays by crystals was studied by **W. L. Bragg** and his father **W. H. Bragg in 1913**. The XRD produced the constructive interference due to the interaction between incident X-ray and the sample according to the Bragg law:

$$\mathbf{2d\sin\theta = n\lambda}$$

Where θ is the Bragg angle, d is interspacing distance between two planes and **λ** is the incident wavelength of the X-ray.

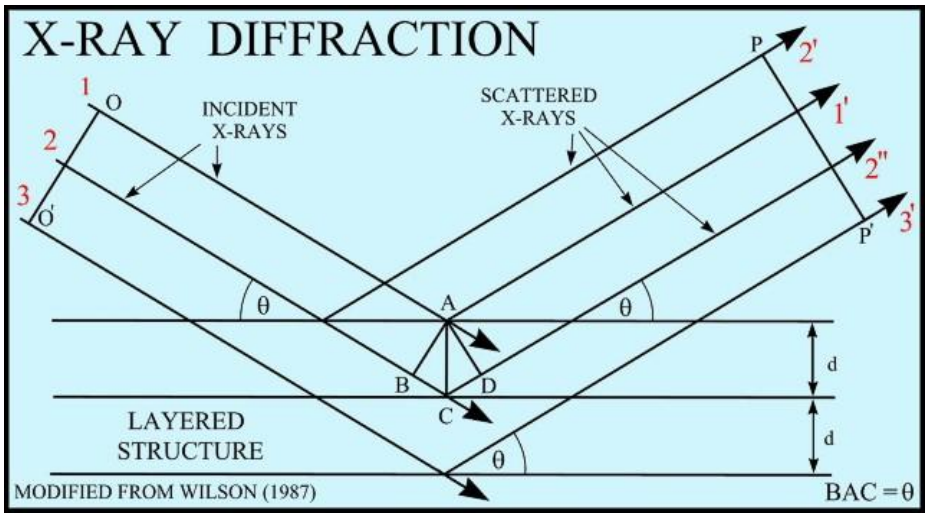


**Fig: 3.2** Schematic of XRD [55]

The Philips X'pert PRO X-ray diffractometer with Cu-$K_\alpha$ radiations having a wavelength of 1.5418 Å was used to analyze the samples. These X-rays are directly incident to the sample and the diffracted rays are collected from the sample. In XRD diffractometer the sample

rotates with an angle θ and the X-ray detector collected the diffracted X-ray across the angle 2θ. The X-ray diffraction can be used to find the crystal structure of an unknown material, crystallite size from analysis of peak broadening, crystallite shape from study of peak symmetry and to determine the degree of crystalline phase.

### 3.2.2 Scanning electron microscope (SEM)

Scanning electron microscope (SEM) is a type of electron microscope that scans the image of sample with a high-energy beam of electrons in a raster pattern. These electrons interact with the atoms of the sample and release signals which contain information about the surface topology, composition, and electrical conductivity of the sample. If the kinetic energies of the incident electrons are extreme high then it can change composition of sample. Therefore for all sample the kinetic energy will be fixed according to the nature of the materials.

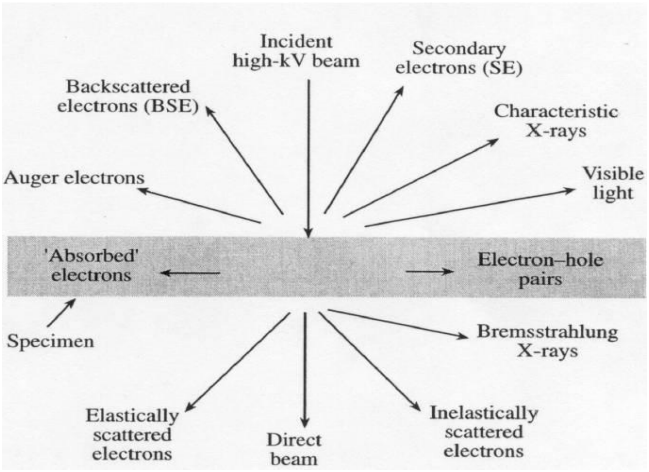


**Fig: 3.3** Interaction of electron with matter [56]

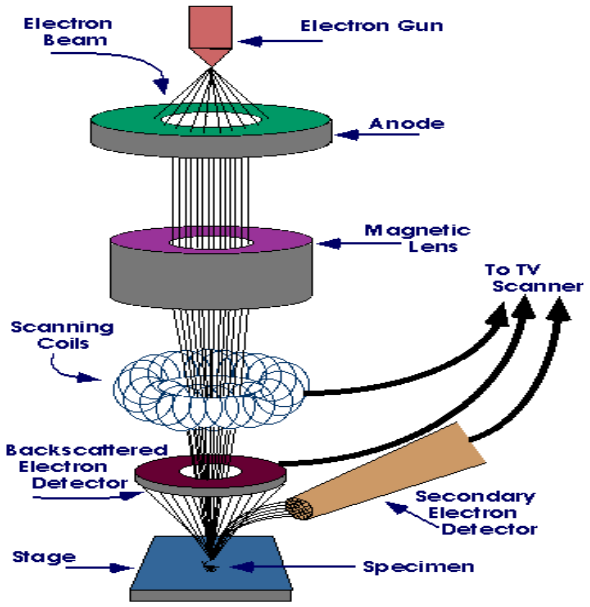


**Fig: 3.4** Schematic diagram of SEM [57]

SEM analysis is considered to be "non-destructive", that is, x-rays generated by electron interactions do not lead to volume loss of the sample, so it is possible to analyse the same materials repeatedly.

### 3.2.3 Vibrating sample magnetometer (VSM)

A vibrating sample magnetometer (VSM) is a scientific instrument that measures magnetic properties of the sample. It was invented in 1955 by Simon Foner. A vibrating sample magnetometer (VSM) set up has pickup coil. If the sample of any material is placed in uniform magnetic field, a dipole moment is induced. If the sample vibrates with sinusoidal motion this induces in suitable pickup coils. The signal has the same frequency of vibration and its amplitude will be proportional to the magnetic moment, amplitude, and relative position with respect to the pick-up coils system. By feeding the signal from the pick-up coil and the reference signal into a demodulator, the magnetic moment of the sample is extracted.

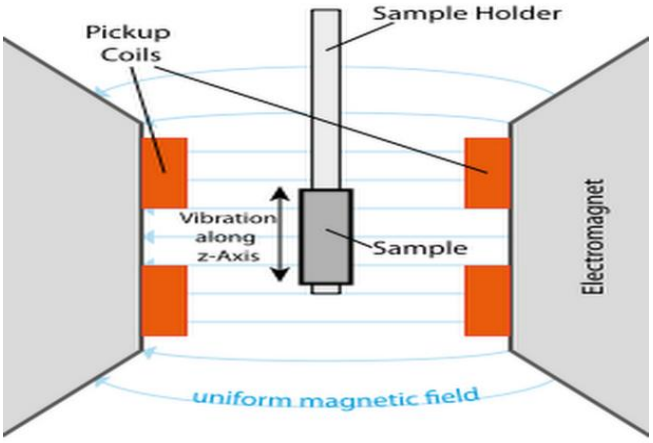


**Fig: 3.5** Schematic illustration of VSM [58]

### 3.2.4 Energy Dispersive X-Ray Spectroscopy (EDS):

EDS is used mainly for elemental analysis and for chemical characterization of samples. All elements from atomic number 4 up to 92 can be detected and analyzed easily by EDX of the sample but elements of low atomic number are difficult to detect.

The major components of EDX setup are beam source, X-ray detector, pulse processor and analyzer. EDX systems are basically used with a SEM as cathode ray energy source and magnetic lenses to create and focus the beam of electrons.

### 3.2.5 P-E loop measurements

The polarization in the material cannot be directly measured by electrical means. However, flowing charge can be measured through external circuits. This forms the basis techniques for the measurement of polarization in the material. The charge can be leakage across the impedance of the voltage measuring instrument because the material is not a perfect insulator. The current will flow through ferroelectric sample. This is a general problem at room temperature.

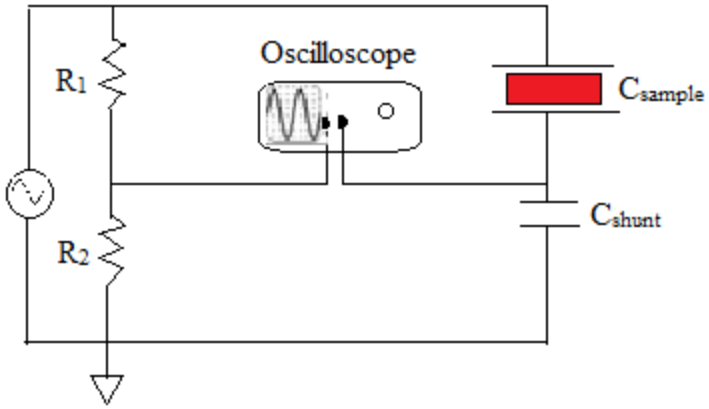


**Fig: 3.6** Schematic diagram of a Shower-Tawer circuit for P-E loop measurement.

The voltage applied across the sample is attenuated by a resistive divider, $R_1$, $R_2$. The sample capacitances, $C_{sample}$, are connected in series with a shunt capacitor $C_{shunt}$ so that the same charge is flowing through the both capacitors. The oscilloscope is connected to measure the voltage across shunt capacitor. A high quality low leakage shunt capacitor provides a stable and linear relationship between charge and voltage so that the measured voltage can be converted to a charge by multiplying the capacitance. Basically, voltages from the resistive divider and shunt capacitor were connected to X and Y plates of cathode ray oscilloscope to generate *P-E* loop.

## CHAPTER 4

## RESULT AND DISCUSSION

### 4.1 XRD analysis

Fig.4.1 displays the XRD pattern of BNT-BKT-BMgT, CZFMO and composite with (X=0.2) sample. XRD patterns of BNT-BKT-BMgT and CZFMO establish the presence of both tetragonal and cubic spinel symmetry respectively. However, XRD of composite sample consist of all the characteristic peaks were indexed as CZFMO and BNT-BKT-BMgT phases.

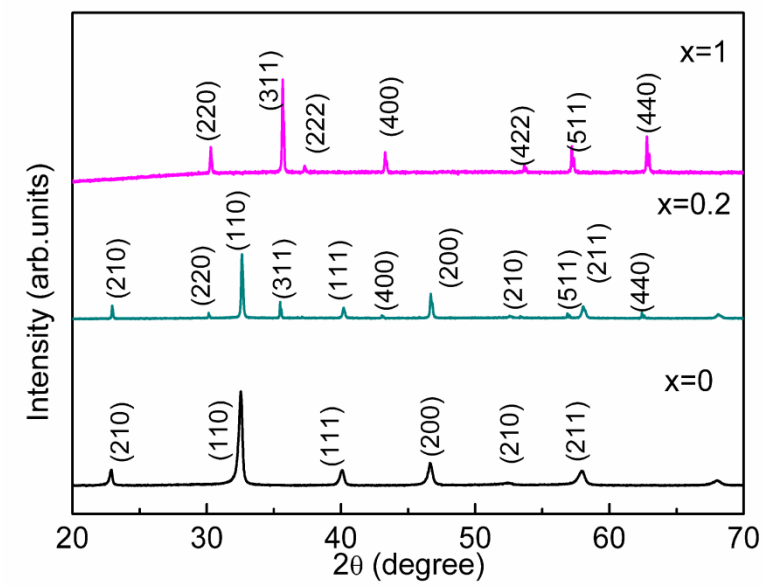


**Fig. 4.1** XRD patterns of (1−*x*)[72.5(BNT)-22.5(BKT)-5(BMgT)] – CZFMO with (*x*=0.0,0.2,1)

No X-ray reflection other than the individual phases were identified, which implies no significant chemical reaction has taken place at the piezoelectric-ferrite interface during the high temperature sintering process, which is essential for proper composite formation.

### 4.2 SEM and EDX analysis

Fig. 4.2 show the SEM micrographs of fracture surface portions of (a) BNT-BKTBMgT, (b) BNT-BKT-BMgT-CZFMO with (x = 0.2) and (c) CZFMO sintered at 900ºC. In case of

particulate composites, the microstructure plays an important role to get the improved Multiferroic properties.

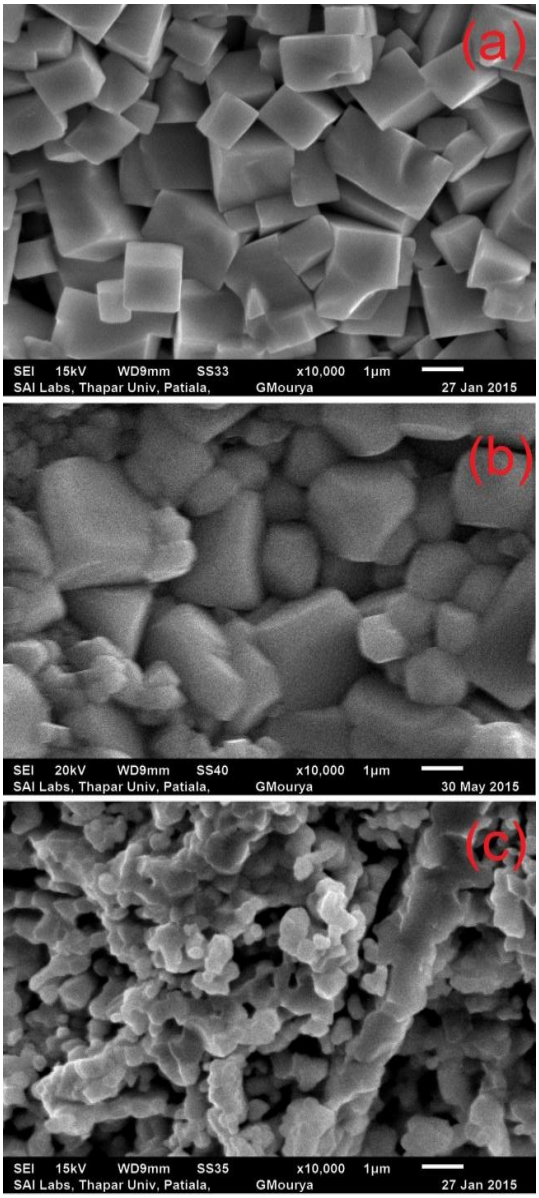


**Fig. 4.2** SEM images of (a) 72.5BNT-22.5BKT-5BMgT (b (1−*x*)[72.5(BNT) 22.5(BKT)-5(BMgT)]−CZFMO (*x*=0.2) and (c) CZFMO

The micrograph suggests the samples were well sintered and dense. The BNT-BKT-BMgT sample shows larger grains as compared to composite sample. The addition of CZFMO promotes reduction in the grain size with little porosity as reported earlier. The reduction in grain size could be the result of pinning action by CZFMO in the composite. The

representative EDX spectra shown in Fig.3 acquired from the area of the sample. The representative EDX spectra confirms the presence of Bi, Na, K, Mg, Ti, Co, Zn, Fe, Mn and O elements in the composite structure.

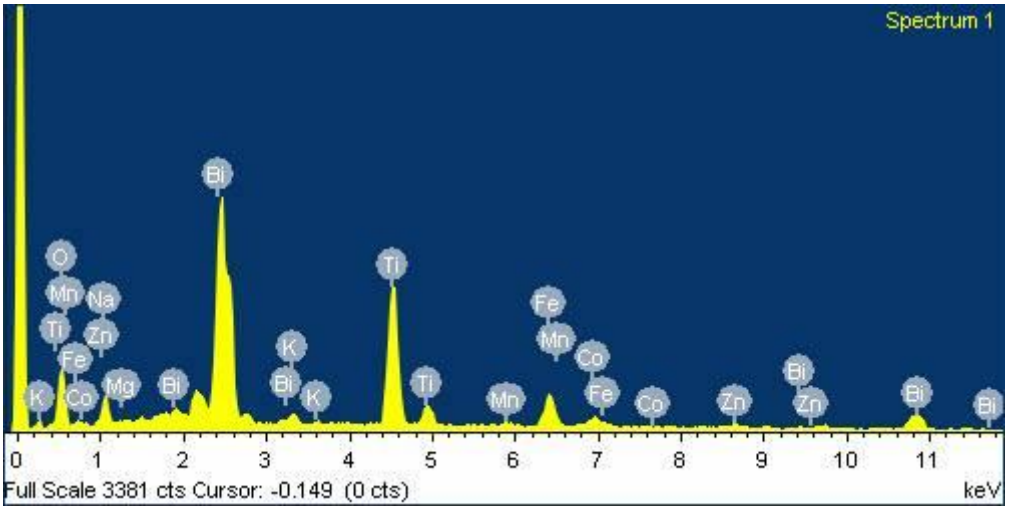


**Fig. 4.3** EDX spectra of (1−*x*)[72.5(BNT)-22.5(BKT)-5(BMgT)] − CZFMO (*x*=0.2)

### 4.3 Ferroelectric properties

Fig. 4.3 shows the *R-T* ferroelectric (*P-E*) loops for samples with (x=0) and composite (x=0.2) measured at 1 Hz frequency. Both BNT-BKT-BMgT and composite with (x=0.2) samples shows well saturated hysteresis loop with large saturation polarization.

The maximum values of saturation polarization ($P_s$ = 29μC/cm$^2$) and ($P_s$ = 16.2μC/cm$^2$) are observed for BNT-BKT-BMgT and composite with (x=0.2) samples. The decrease values of saturation polarization *(Ps)* for composite sample are observed due to the low resistivity of ferrite phase. The increased $E_c$ of the composite is due to the pinning effect of CZFMO.

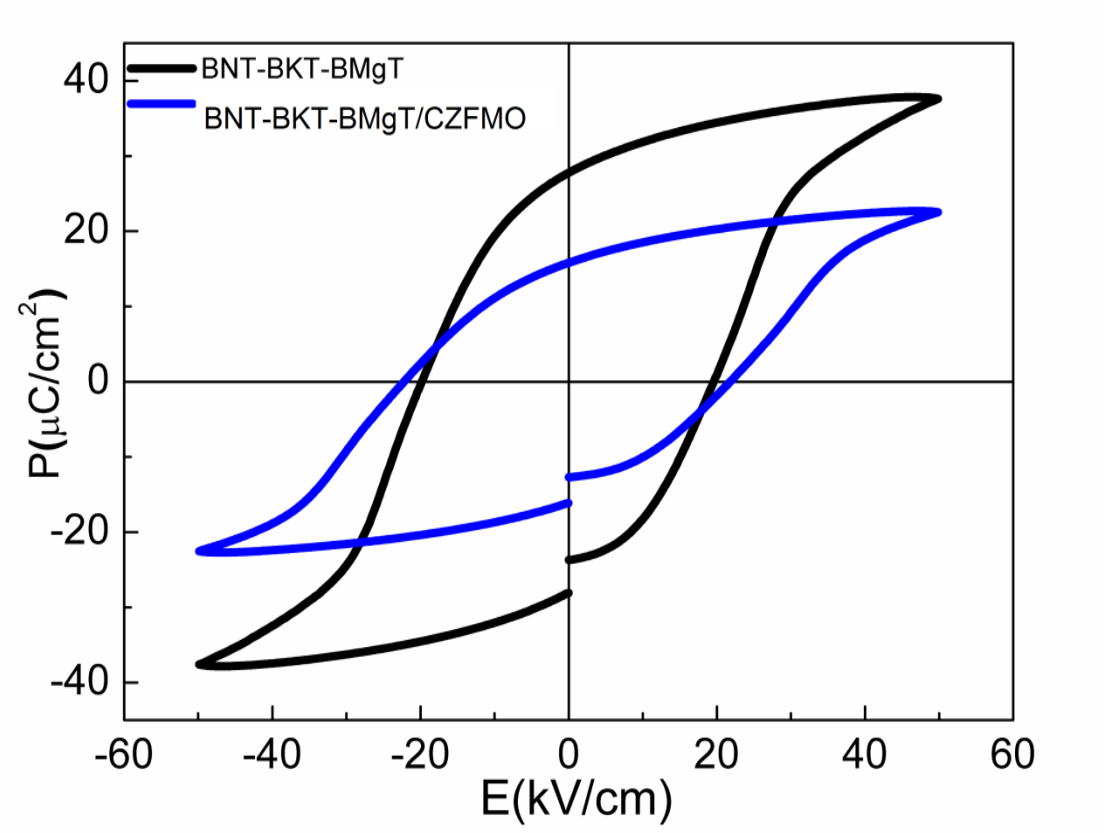


**Fig. 4.4** *P-E* loops of (a) (1−*x*)[72.5(BNT)-22.5(BKT)-5(BMgT)] − CZFMO (*x*=0.0, 0.1,0.2, 0.3). Inset: variation of $P_r$ and $E_c$ are plotted as a function of increasing CZFMO content.

### 4.4 Magnetic properties

Fig.4.5 shows the *M-H* loops (a) for pure sintered CZFMO and (b) composite with (x=0.2). The well saturated *M-H* loop indicates the ferromagnetic nature of the samples. The saturation magnetization ($M_s$) and remnant magnetization ($M_r$) decreased with the decrease of ferrite content. The values of $M_s$ for pure CZFMO and composite with (0.2) were found to be ~ 81emu/g and 14emu/g respectively. Also, as shown in zoom view of fig. 4.5 the coercive field were found to be increased for composite sample. The values for $H_c$ is increased from ~26Oe for pure CZFMO to ~48Oe for composite with (x=0.2). The low corecivity of the samples confirmed the soft magnetic nature of the sample.

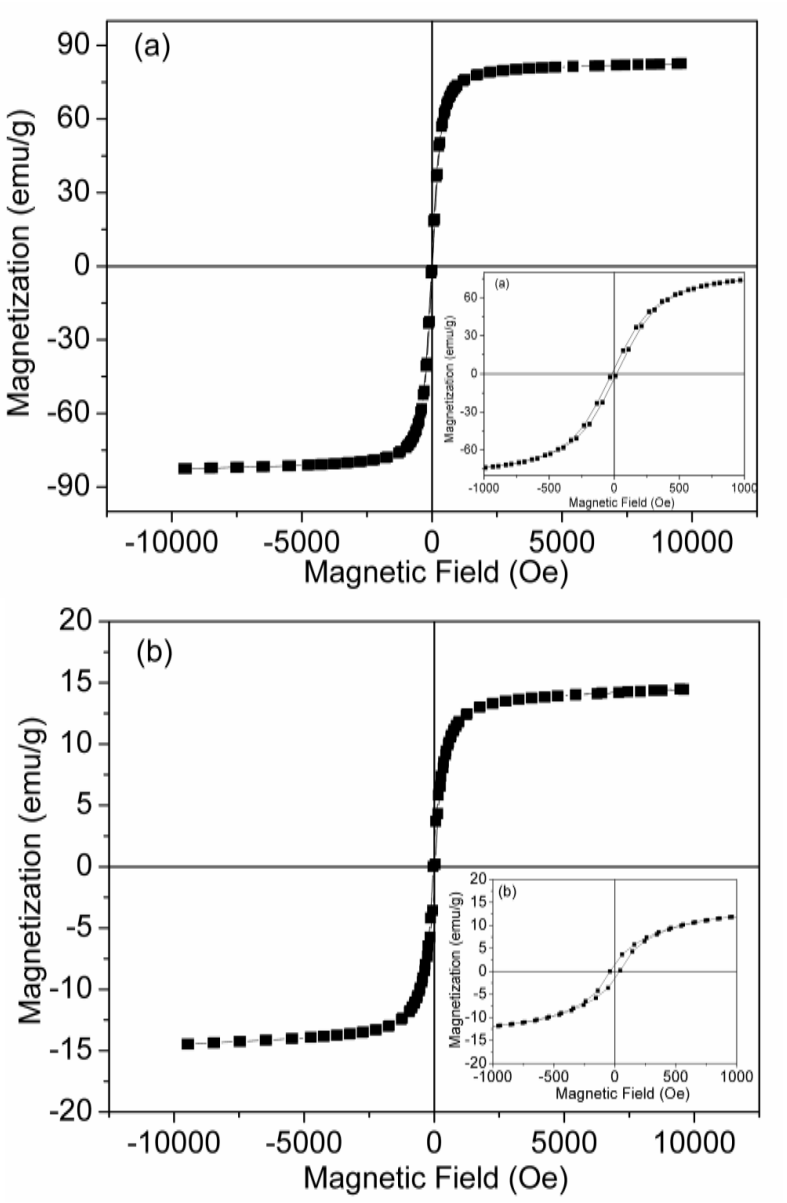


**Fig. 4.5** The *M-H* loop of (1−*x*)[72.5(BNT)-22.5(BKT)-5(BMgT)] − CZFMO (x=0.2) and the inset is zoom view of the central part of the figure.

## 4.5 Conclusions

- Pure BNT-BKT-BMgT and CZFMO and composite material has been prepared by sol-gel method. Further, ME particulate composites of (1-x) BNT-BKT-BMgT – (x) CZFMO (x=0.2) has been prepared.
- All the peaks of composite sample are indexed to CZFMO and BNT-BKT-BMgT. No chemical reaction was observed at the piezoelectric-ferrite phase during the high temperature sintering process.
- The morphology of pellets of pure BNT-BKT-BMgT and CZFMO and composite (BNT-BKT-BMgT-CZFMO) sintered at 900°C shows the larger grain size of BNT-BKT-BMgT as compared to composite sample. The grain size reduces with a little porosity by adding the CZFMO.
- Presence of Bi, Na, K, Mg, Ti, Co, Zn, Fe, Mn and O elements in the composite structure are confirmed by EDX spectrum.
- Ferroelectric behaviour of pure BNT-BKT-BMgT and composite, polarization as function of electric field *(P-E)* measurements was carried out. Both the samples show well saturated hysteresis loop with saturation polarization. The maximum value of saturation polarization for BNT-BKT-BMgT and composites are observed $P_s$ = 29 μC/cm$^2$ and $P_s$ = 16.2 μC/cm$^2$ respectively.
- The value of magnetic saturation of $M_s$ for pure CZFMO and composite found to be ~ 81emu/g and ~ 14 emu/g respectively.

**References**


1. C. W. Nan, M. I. Bichurin, S.Dong, D. Viehland, and G. Srinivasan, J.of Appl. Phys. **103**, 031101 (2008).
2. R. Ramesh and N. A. Spaldin, Nat. Mater. **6,** 21(2007).
3. J. F. Scott and C. A. Paz de Araujo, Sci. **246**, 1400 (1989).
4. J. F. Scott, Nat. Mater. **6**, 256 (2007).
5. G. A. Prinz, Sci. **282,** 1660 (1998).
6. H. Schmid, Ferroelectrics **162**, 665(1994).
7. C. Chappert, A. Fert, and F. N. Van Dau, Nat. Mater. **6**, 813 (2007).
8. Y. wang, J. Hu, Y. Lin, C.W. Nan, NPG Asia Mater. **2**, 61 (2010)
9. L.W. Martin, Dalton Trans **39**, 10813 (2010).
10. M. Fiebig, J. of Phys. D: Appl. Phys. **38**, 123 (2005)
11. W. Eerenstein, N. D. Mathur, and J. F. Scott, Nature London **442**, 759 (2006).
12. D. I. Khomskii, J. Magn. Magn. Mater. **306,** 1 (2006).
13. S. W. Cheong and M. Mostovoy, Nat. Mater. **6**, 13 (2007).
14. J. P. Velev, S. S. Jaswal, and E. Y. Tsymbal, Phil. Trans. R. Soc. A **369**, 3069 (2011).
15. W. Prellier, M. Singh and P. Murugavel, J. Phys.: Condens. Matter. **17**, 803 (2005).
16. Y. Tokura and N. Kida, Phil. Trans. R. Soc. A **369**, 3679(2011)
17. G. Laws and G. Srinivasan, J. Phys. D: Appl. Phys. **44**, 243001 (2011).
18. L. D. Landue and E. Lifshitz, Addison-Wesley, Reading, Mass, USA, (1960).
19. I. O. Troyanchuk et al, J. Phys. Condens. Matter **8,** 11205 (1996).
20. Z. J. Huang, Y. Cao, Y. Y. Sun, Y. Y. Xue, C. W. Cue, Phys. Rev. B **56**, 2623 (1997).

21. T. Kimura, S. Kawamoto, I. Yamada, M. Azuma, M. Takano, Y. Tokura, Phys. Rev. B **67,** 180401(2003).

22. D. Ito, N. Fujimura, T. Yoshimura, T. Ito, J. Appl. Phys. **93,** 5563 (2003).

23. T. H. Kim, S. H. Baek, S. M. Yang, S. Y. Jang, D. Ortiz, T. K. Song, J.S. Chung, C. B. Eom, T. W. Noh, and J.G. Yoon ,Appl. Phys. Lett. **95,** 262902 (2009).

24. D. Pantel,Y. H. Chu,L. W. Martin, R. Ramesh, D. Hesse, M. Alexe, J. Appl. Phys. **107,** 084111(2010).

25. D. Khomskii, Phys. **20**, 2 (2009).

26. D. V. Efremov, J. V. Brink, D. I. Khomskii, Nat. Mater. **3**, 853 (2004).

27. B. B. Van Aken, T. T. M. Palstra, A. Filippetti & N. A. Spaldin, Mater. **3**, 164 (2004).

28. H. C. He, J. P. Zhou, J. Wang, and C. W. Nan, Appl. Phys. Lett. **89**, 052904 (2006).

29. H. Ryu, P. Murugavel, J. H. Lee , S. C. Chae, and T. W. Noha, Y. Seok Oh, H. J. Kim, K. H. Kim, J. H. Jang, M. Kim, C. Bae , J.G. Park Appl. Phys. Lett. **89,** 102907(2006).

30. Y. G. Ma, W. N. Cheng, M. Ning, and C. K. Ong, Appl. Phys. Lett. **90**, 152911 (2007).

31. J. V. Boomgard and R. A. Born, J. Mat. Sci. **13**, 1538 (1978).

32. S. N. Babu, J. H. Hsu, Y. S. Chen, J. G. Lin, J. Appl. Phys. **109**, 07D904 (2011).

33. S. N. Babu, L. Malkinski, J. Appl. Phys. **111**, 07D919 (2012).

34. A. Gupta, A. Huang, S. Shannigrahi, R. Chatterjee, App. Phys. Lett. **98**, 112901 (2011).

35. A. Gupta, R. Chatterjee, J. Europ. Ceram. Soc. **33,** 1017(2013).

36. http://122.physics.ucdavis.edu/?q=node/34.

37. B. Jaffe, W. R. Cook, H. Jaffe: Piezoelectric ceramics, Academic Press, London, 49 (1971).

38. B. D. Cullity: Introduction to Magnetic Materials, Addison Wesley, Reading, MA, 185 (1972).

39. I. E. Dzyaloshinskii, Sov. Phys. JETP **10**, 628 (1960).

40. D. N. Astrov, Sov. Phys. JETP **11**, 708 (1960).

41. Y. Lin, N. Cai, J. Zhai, G. Liu, and C. W. Nan, Phys. Rev. B **72**, 012405 (2005).

42. J. Ryu, A. V. Carazo, K. Uchino, H. E. Kim, J. Electroceram. **7**, 17 (2001).

43. J. Zhai, N. Cai, Z. Shi, Y. Lin and C. W. Nan, J. Phys. D: Appl. Phys. **37**, 823 (2004).

44. J. Zhai, N. Cai, Z. Shi, Y. Lin, and C. W. Nan, J. of Appl. Phys. **95**, 5685 (2004).

45. L. Weng, Y. Fu, S. Song, J. Tang, J. Li, Scripta Mater. **56,** 465 (2007).

46. G. Srinivasan, E. T. Rasmussen, J. Gallegos, and R. Srinivasan, Phys. Rev. B **64**, 214408 (2011).

47. J. Zhou, H. He, Z. Shi, G. Liu, and C. W. Nan, J. of Appl. Phys. **100**, 094106 (2006).

48. S. K. Upadhyay and V. R. Reddy, J. of Appl. Phys. **113**, 114107 (2013).

49. A. Srinivas, R. V. Krishnaiah, T. Karthik, P. Suresh, Saket Asthana, and S. V. Kamat, Appl. Phys. Lett. **101**, 082902 (2012).

50. D.K. Pradhan, S. K. Barik, S. Sahoo, V. S. Puli, and R. S. Katiyar, J. of Appl. Phys. **113**, 144104 (2013).

51. N. Adhlakha and K. L. Yadav, Smart Mater. Struct. **21,** 115021 (2012).

52. A. D. Sheikh, A. Fawzi, V.L. Mathe, J. Magn. Magn. Mater. **323**, 740 (2011).

53. G. Sreenivasulu, V. H. Babu, G. Markandeyulu, and B. S. Murty, Appl. Phys. Lett. **94**, 112902 (2009).

54. E. V. Ramana, F. Figueiras, M. P. F. Graçaa and M. A. Valentea, Dalton Trans. **43**, 9934 (2014).

55. http://pubs.usgs.gov/of/2001/of01-041/htmldocs/xrpd.htm].

56.[http://www.globalsino.com/micro/1/1micro9740.html].

57.[https://www.purdue.edu/ehps/rem/rs/sem.htm].

58. https://en.wikipedia.org/wiki/Vibrating_sample_magnetometer.